

## **Synergistic Bio-Inspired Photocatalytic Hydrogen Production by Chlorophyll Derivative Sensitized Nb<sub>2</sub>CT<sub>x</sub> MXene Nanosheets**

Tianfang Zheng,<sup>a</sup> Lin Yang<sup>\*,b</sup>, Hai Xu,<sup>c</sup> Aijun Li,<sup>a</sup> Shin-ichi Sasaki,<sup>d</sup> and Xiao-Feng Wang<sup>\*,a</sup>

*<sup>a</sup> Key Laboratory of Physics and Technology for Advanced Batteries (Ministry of Education), College of Physics, Jilin University, Changchun 130012, People's Republic of China.*

*<sup>b</sup> Key Laboratory for UV-Emitting Materials and Technology of Ministry of Education, Northeast Normal University, Changchun 130024, Jilin, China*

*<sup>c</sup> College of Chemistry, Jilin University, Changchun 130012, People's Republic of China.*

*<sup>d</sup> Faculty of Bioscience, Nagahama Institute of Bio-Science and Technology, Nagahama, Shiga 526-0829, Japan*

## Experimental section

**Synthesis of Chl and monolayer Nb<sub>2</sub>CT<sub>x</sub> MXene:** Methyl *trans*-3<sup>2</sup>-carboxy-pyropheophorbide-*a* (**Chl**) was synthesized as previously reported.<sup>1</sup> For the preparation and delamination of Nb<sub>2</sub>CT<sub>x</sub> MXene, the HF etching and tetramethylammonium hydroxide (TMAOH) intercalation method was used. 3 g Nb<sub>2</sub>AlC MAX phase powder was added into aqueous 49 wt% HF solution (50 mL) in small portions. The whole process was completed in two minutes. Then, the resulting suspension was stirred at 350 rpm at 55 °C for 72 h. After that, the supernatant was removed and the precipitate was washed with deionized (DI) water until the supernatant reached to nearly neutral. The sediment was collected and dried in a vacuum oven for 12 hours. Then it was completely grounded into a fine powder, and the resulting powder was stirred with ascorbic acid (AA) in DI water until uniformly dispersed (1 g powder / 0.2 g AA / 10 mL DI water). 20 mL TMAOH per gram powder was slowly added into the above suspension with continuous stirring for 20 minutes. The mixture was transferred into a 100 mL PTFE hydrothermal autoclave reactor liner and pumped with Ar for 15 min. The assembled hydrothermal autoclave reactor was heated to 160 °C and maintained for 24 h and then cooled naturally to room temperature. After poured off the upper portion of the clarified solution in the liner, DI water was added to the precipitate, suspended, and centrifuged to wash it several times. The combined upper solution was ultrasonicated for 1 h. After treatment, it was dried in a vacuum oven to obtain monolayer of Nb<sub>2</sub>CT<sub>x</sub> MXene.

**Synthesis of Chl@Nb<sub>2</sub>CT<sub>x</sub> Composites:** To investigate the effect of the mass ratio between Nb<sub>2</sub>CT<sub>x</sub> as a co-catalyst and **Chl** as sensitizer on the photocatalytic activity, a series of composites with different mass ratios were synthesized as follows: A stock solution of **Chl** in tetrahydrofuran (THF) was prepared at a concentration of 1 mg/mL, and it was added to 3 mg of Nb<sub>2</sub>CT<sub>x</sub> according to different mass ratios (e.g., 2 wt% **Chl** is taken as 60 μL of solution). The resulting mixture was protected from light and stirred to dryness at 350 rpm at room temperature, and the remaining powder was collected and stored away from light.

**Characterization:** X-ray diffraction (XRD) patterns were measured with a Cu K $\alpha$  radiation (Bruker, D8). Scanning electron microscope (SEM, Hitachi, Regulus 8100) and transmission electron microscope (TEM, JEOL, JEM-2200FS), and Fourier Transform Infrared Spectrometer (FT-IR, Bruker, VERTEX 80v) were used to observe the different microstructures of the samples. Ultraviolet–visible (UV–vis) spectra were recorded on UV-3100 spectrophotometers (Shimadzu, Japan). Cyclic voltammograms (CV), photocurrent responses, and electrochemical impedance spectroscopy (EIS) measurements as well as the Mott-Schottky tests were carried out with CHI760E electrochemical workstation (CH Instruments, China).

**Photochemical Performance:** EIS and time-dependent photocurrent (TPC) responses were carried out on a typical three-electrode system with 0.5 M Na<sub>2</sub>SO<sub>4</sub> as electrolyte. The composite was dispersed in the mixed solution of DI water and anhydrous ethanol containing Nafion. The mixture was coated on fluorine-doped tin oxide glass.

**Photocatalytic Performance:** In this work, we used photocatalytic hydrogen evolution as a probe reaction to investigate the photocatalytic performance of the Chl@Nb<sub>2</sub>CT<sub>x</sub> composite. Each photocatalyst (3 mg) was used in the experiment and it was mixed in a 55 mM aqueous solution of AA (3 mL). After ultrasonication for 5 min and purging with Ar gas for 15 min, the suspension was irradiated under Xe lamp ( $\lambda > 420$  nm) with stirring. AA served as the sacrificial agent to regenerate Chl sensitizers during the reaction by reducing the remaining holes on Chl molecules after injection the photogenerated electrons into Nb<sub>2</sub>CT<sub>x</sub> MXene. The reaction progress was monitored by analyzing the volume of hydrogen gas generated over time using gas chromatography (GC). Gas samples were taken per hour and analyzed utilizing a 5 Å molecular sieve column and TCD.

#### **Details for Mott-Schottky tests**

As delineated by the Mott-Schottky equation:

$$\frac{1}{C_{SC}^2} = \frac{2}{Ne_0\epsilon_0\epsilon_r} \left( E - E_{FB} - \frac{kT}{e} \right)$$

where  $C_{SC}$  is space-charge capacitance,  $N$  is the carrier concentration,  $\epsilon_0$  is vacuum dielectric constant,  $\epsilon_r$  is the relative dielectric constant,  $E_{FB}$  is flat band voltage,  $k$  is Boltzmann constant, and  $T$  is thermodynamic temperature, respectively. According to the above equation, then the carrier concentration in the light state is named as  $N_L$  and the carrier concentration in the dark state is named as  $N_D$ , and the ability of **Chl** as a photocatalyst to produce photogenerated carriers under light can be obtained by comparing  $\frac{N_L}{N_D}$ . As a result,  $\frac{N_L}{N_D}$  of **Chl@Nb<sub>2</sub>CT<sub>x</sub>** was calculated to be 1.23, indicating a massive photogenerated carrier production.

Table. S1 UV-vis absorption peaks of **Chl** in THF and **Chl@Nb<sub>2</sub>CT<sub>x</sub>** film.

	<b>Soret Band</b>	<b>Q<sub>x</sub> Band</b>	<b>Q<sub>y</sub> Band</b>
<b>Chl</b> in THF	416 nm	514 nm; 543 nm	621 nm; 681 nm
<b>Chl@Nb<sub>2</sub>CT<sub>x</sub></b> film	436 nm	576 nm; 618 nm	686nm; 744nm

The positions of the characteristic absorption peaks of **Chl** and **Chl@Nb<sub>2</sub>CT<sub>x</sub>** are listed in Table. S1, and it can be seen that after the formation of the film, the characteristic absorption peaks of **Chl** undergo a significant redshift and broadening. The Soret band, observed at shorter wavelengths, originates from a robust transition from the ground state (S0) to the second excited state (S2), denoted as S0 → S2. This transition involves molecular orbitals of the porphyrin ring, particularly a  $\pi \rightarrow \pi^*$  transition, where electrons are excited from the highest occupied molecular orbital (HOMO) to the lowest unoccupied molecular orbital (LUMO), representing a transition to the second excited state. The prominence of the Soret band underscores the strong absorption associated with this transition. Conversely, the Q band, situated at longer wavelengths, corresponds to a more subdued transition from the ground state (S0) to the first excited state (S1), denoted as S0 → S1.

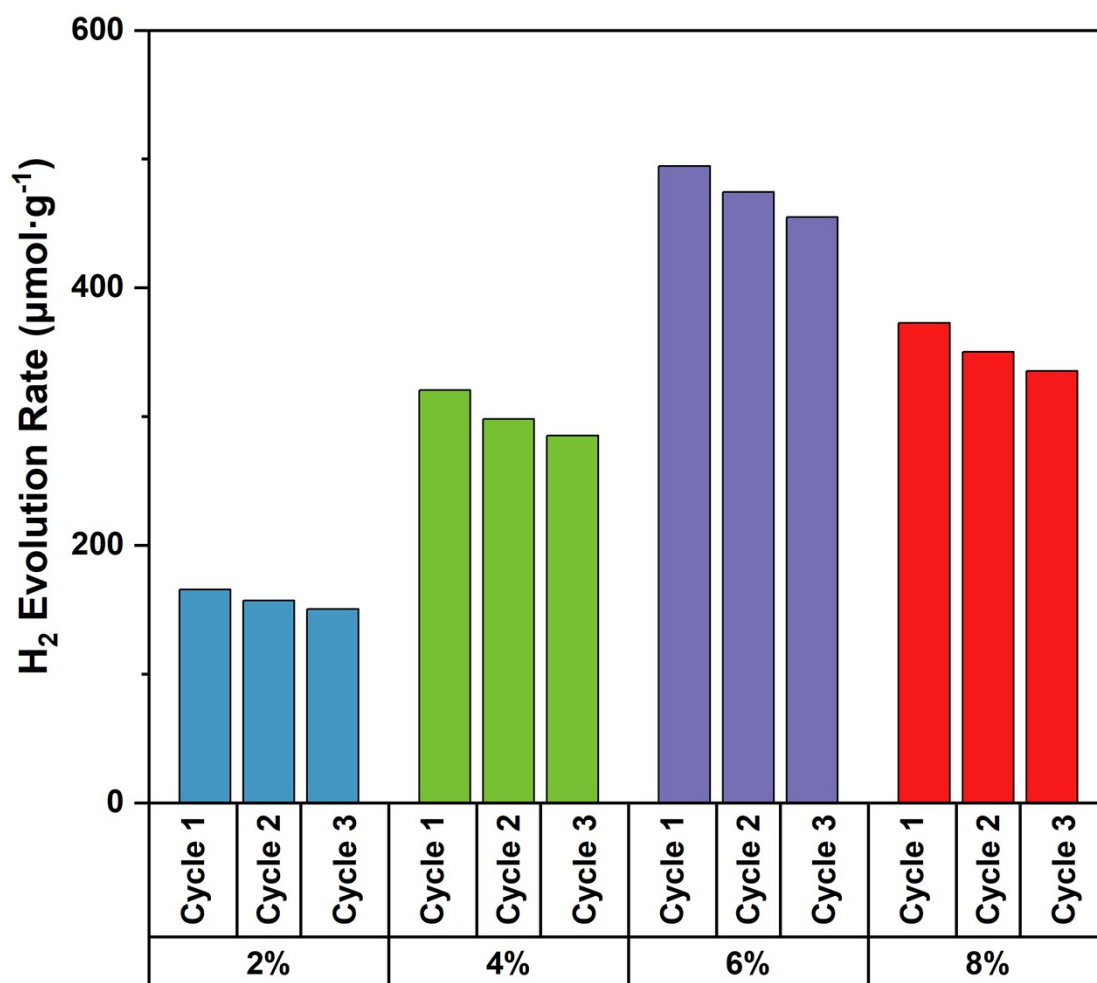


Figure S1 Stability of  $\text{Chl@Nb}_2\text{CT}_x$  with different for hydrogen evolution.

The stability of the hydrogen evolution of  $\text{Chl@Nb}_2\text{CT}_x$  with different ratios is given in Figure S1. It can be seen that the samples with different **Chl** ratios have relatively excellent stability, and the stability is not greatly affected by the **Chl** ratio. Specifically, the composite containing 2% **Chl** maintains 91% stability after three cycles, the composite containing 4% **Chl** maintains 93%, the composite containing 6% **Chl** maintains 92%, and the composite containing 8% **Chl** maintains 90%.

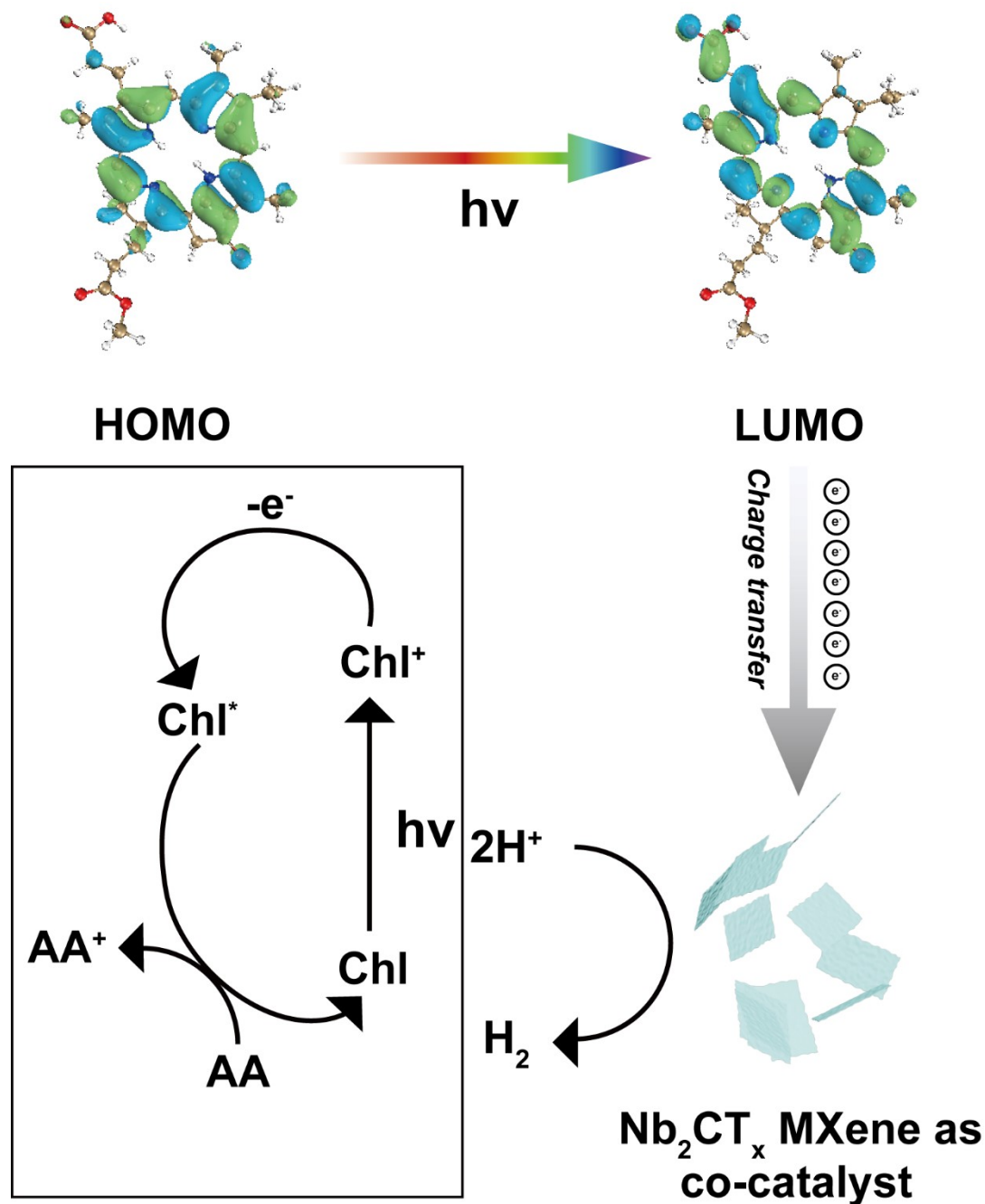


Figure S2 Schematic diagram of the working mechanism of the photocatalytic system in this work.

A proposed working mechanism is given in Figure S2. After combining with Nb<sub>2</sub>CT<sub>x</sub> as a co-catalyst to form a composite photocatalytic system, the problem of electron-hole recombination in the excited state **Chl** molecule was well solved. Moreover, the results of the wave function distribution obtained by DFT calculations showed that upon excitation, the photogenerated electrons in **Chl** preferred to be distributed near the carboxy group at the C3<sup>2</sup> position, and it was this group that was

combined with Nb<sub>2</sub>CT<sub>x</sub> through interactions, a finding that further demonstrated the excellent potential of the composite photocatalytic system.<sup>2</sup>

Photocatalytic System	Illumination	HER Efficiency	Ref.
Chl@Cu <sub>2</sub> O/Ti <sub>3</sub> C <sub>2</sub> T <sub>x</sub>	$\lambda > 420$ nm	174 $\mu\text{mol/g/h}$	[3]
Chl@g-C <sub>3</sub> N <sub>4</sub> /Ti <sub>3</sub> C <sub>2</sub> T <sub>x</sub>	$\lambda > 420$ nm	131 $\mu\text{mol/g/h}$	[4]
Squaraine/Ti <sub>3</sub> C <sub>2</sub> T <sub>x</sub>	$\lambda > 420$ nm	28.6 $\mu\text{mol/g/h}$	[5]
Chl/Ti <sub>3</sub> C <sub>2</sub> T <sub>x</sub>	$\lambda > 420$ nm	87 $\mu\text{mol/g/h}$	[6]
Chl/ <i>m</i> -Ti <sub>3</sub> C <sub>2</sub> T <sub>x</sub>	$\lambda > 420$ nm	106 $\mu\text{mol/g/h}$	[7]
BChl/Ti <sub>3</sub> C <sub>2</sub> T <sub>x</sub>	$\lambda > 420$ nm	15.5 $\mu\text{mol/g/h}$	[8]

## Reference

- 1 X.-F. Wang, O. Kitao, H. Zhou, H. Tamiaki and S. Sasaki, *Chem. Commun.*, 2009, 1523–1525.
- 2 T. Lu and F. Chen, *J. Comput. Chem.*, 2012, **33**, 580–592.
- 3 Y. Li, Y. Liu, T. Zheng, A. Li, G. G. Levchenko, W. Han, A. V. Pashchenko, S. Sasaki, H. Tamiaki and X.-F. Wang, *Green Chem.*, 2024, **26**, 1511–1522.
- 4 Y. Li, Y. Liu, T. Zheng, Z. Liu, G. G. Levchenko, W. Han, A. V. Pashchenko, S. Sasaki, H. Tamiaki and X.-F. Wang, *Appl. Surf. Sci.*, 2023, **640**, 158454.
- 5 Y. Liu, Y. Li, A. Li, Y. Gao, X.-F. Wang, R. Fujii and S. Sasaki, *J. Colloid Interface Sci.*, 2023, **633**, 218–225.
- 6 T. Zheng, Y. Li, Y. Sun, Y. Dall’Agnese, C. Dall’Agnese, S. Sasaki, H. Tamiaki and X.-F. Wang, *Energy Technology*, 2022, **10**, 2100713.
- 7 Y. Li, Y. Liu, T. Zheng, S. Sasaki, H. Tamiaki and X.-F. Wang, *J. Photochem. Photobiol. A*, 2022, **427**, 113792.
- 8 X. Sun, Y. Li, X.-F. Wang, R. Fujii, Y. Yamano, O. Kitao and S. Sasaki, *New J. Chem.*, 2022, **46**, 2166–2177.